ELSEVIER

Journal of Alloys and Compounds 253–254 (1997) 467–470

Journal of ALLOYS AND COMPOUNDS

The influence of hydrogen on the growth of yttrium on Ni(001) and Ni(110)

D. Naumović*, P. Spatz, J. Hayoz, P. Aebi, L. Schlapbach

Institut de Physique, Université de Fribourg, Pérolles, CH-1700 Fribourg, Switzerland

Abstract

The influence of hydrogen on the growth of Y on Ni(001) and Ni(110) at room temperature is studied by full-hemispherical X-ray photoelectron diffraction and X-ray photoelectron spectroscopy. We find that Y starts to form a hydride at a thickness of about 25 Å when evaporating Y under a 10^{-6} mbar hydrogen partial pressure. At the same time a weak ordering of the hydride on Ni is observed in the form of a preferential orientation. No ordering occurs for evaporation without hydrogen in ultra-high vacuum.

Keywords: Hydrogen; Yttrium; Nickel; Growth; Full-hemispherical photoelectron diffraction

1. Introduction

Not much is known on the Y/Ni system. To our knowledge it has not been investigated before. It is of interest as a model system to study the influence of hydrogen on the growth process. Y forms, very easily, different hydrides and promises to show a change in behaviour when grown under a partial pressure of H_2. Hydride formation varies the crystalline structure and the lattice constant and therefore the lattice-mismatch conditions. Ni is a magnetic material and in case of Ni/YH_x/Ni sandwich structures one might think of possible fine-tuning of the magnetic coupling by means of varying the hydrogen partial pressure. While this may still be wishful thinking, we will present here the first measurements on thin Y-layers deposited on Ni(001) and Ni(110) single crystals using the full-hemispherical X-ray photoelectron diffraction (XPD) technique. We find a distinct influence of hydrogen on the growth of both crystals.

In the Section 2 a brief introduction to the method is given together with the details of the experiment. The results and discussion section follows before we conclude.

2. Experimental

XPD is by now a well-established chemically-sensitive technique for surface-structure determination of single crystals. It is based on X-ray photoemission spectroscopy (XPS). The photon is absorbed via the photoelectric effect and since the atomic species have characteristic electron binding energies, photoelectrons are detected at different kinetic energies. Distinct species are therefore easily distinguishable. It is then possible to select photoelectrons originating from a particular type of atom. Intensity changes not only due to the concentration of the species, but also because of interference of the outgoing electron wave with its, from neighbouring atoms, scattered wave as a function of angle. Depending on the arrangement of the atoms near the emitting atom and the kinetic energy of the photoelectron, interference occurs to be constructive or destructive. The photon energy used in the present experiment ($h\nu$=1253.6 eV) is such that the kinetic energy of photoelectrons from the core level examined is above 500 eV, namely Y $3d_{5/2}$ at 1097 eV and Ni 3p at 1187 eV (not shown). For this energy regime, the main scattering intensity occurs in forward direction [1]. Therefore, the mapping of the core-level intensity over the hemisphere above the single-crystal sample surface results in a projection of the atom–atom directions starting from the emitter corresponding to the core level under consideration. [2] The observed pattern does not so much depend anymore on the chemical species of the scatterers, the atomic number or the exact kinetic energy, but mainly on the local crystallographic arrangement around the emitter. The diffractogram obtained from a particular emitter is therefore very specific and unique to its local real-space environment.

*Corresponding author.

0925-8388/97/$17.00
PII S0925-8388(96)03095-2

The fact that the technique is surface sensitive and provides information on the local environment of an emitter is due to the relatively short mean free path of the photoelectron. At these energies its value lies between about 10 and 50 Å.

Experimentally, the data acquisition is fully automatized. The X-ray source and electron-energy analyzer are fixed while the sample is rotated. Motorized sequential data collection starts at grazing emission angles and the number of azimuthal settings is chosen such that the solid angle above the specimen is sampled with equal density giving a total of more than 4000 polar and azimuthal angular (θ,φ)-settings for the measurements presented here. The different data points are plotted using the stereographic projection. Grazing emission angles (polar angles) are plotted towards the exterior, and 90° off-normal emission is represented by the outer circle. Normal emission is found at the center. A linear gray scale with 256 levels is used for the intensities, with white and black for maximal and minimal intensities, respectively.

Sample preparation and photoemission experiments were performed in a VG ESCALAB Mark II ultra-high vacuum spectrometer modified in order to enable motorized sequential angle-scanning data acquisition [2] with a base pressure in the 10^{-11} mbar range. Clean Ni(001) and Ni(110) surfaces were prepared by repeated cycles of Ar^+ sputtering and short annealing up to approximately 600 °C. After this treatment, low-energy electron diffraction (LEED) showed well-defined and sharp spots indicating well-ordered surfaces. Y films were evaporated from a liquid-nitrogen cooled source with an electron-bombardment heating. The pressure did not exceed 5×10^{-9} mbar during Y evaporation. The evaporation rate was monitored with a water-cooled quartz micro balance and was approximately 3–6 Å min^{-1} for the thinner films and 12 Å min^{-1} for the thicker films. All films were deposited at room temperature. Surface contamination and film thickness were checked with XPS. Preparation of the Y film, recording of the XPD maps and XPS spectra did not exceed a typical time of five hours, such that contaminations could be kept as low as possible. The different emission lines were measured by integrating the intensity on the peak maximum and subtracting the background intensity measured in front of the peak. Typically, intensity was accumulated for several seconds on each emission line before moving to the next angular setting.

3. Results and discussion

Fig. 1 shows the photoemission intensity in the region of the Y 3d photoemission line as a function of electron binding energy for different Y films evaporated on Ni(110) at room temperature. Photoelectrons were excited with Mg Kα radiation ($h\nu$=1253.6 eV). The bottom-most two

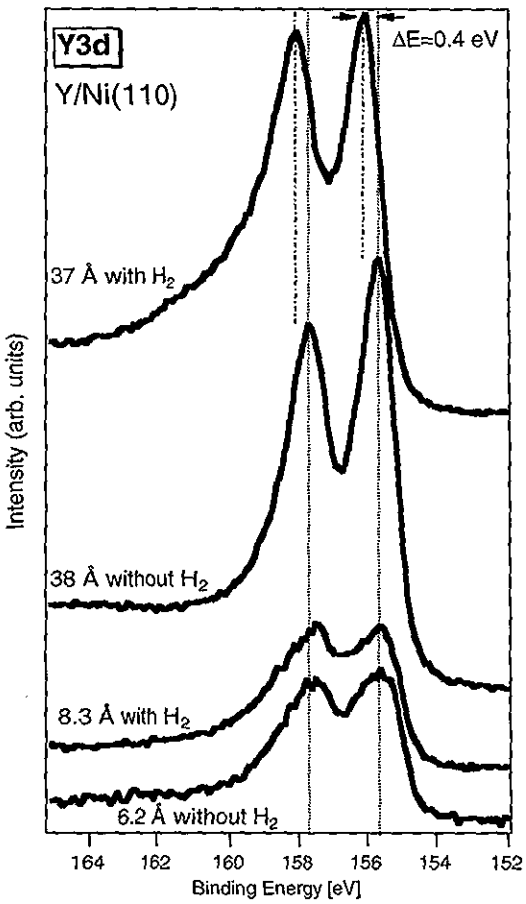

Fig. 1. Y 3d XPS spectrum for thin and thick Y films deposited with and without a 10^{-6} mbar H_2 partial pressure. Note that only the thick film exhibits a chemical shift when deposited under H_2.

curves show the spectra for two thin Y films evaporated with and without a H_2 partial pressure of 10^{-6} mbar. The two curves are virtually identical, indicating that hydrogen did not influence the chemical environment of Y atoms as seen from identical energy positions of the Y 3d doublet compared with the thicker Y film deposited without H_2 partial pressure (third curve from bottom). However, when such a 37 Å thick film is grown under a H_2 partial pressure of 10^{-6} mbar, a chemical shift of 0.4 eV towards higher binding energies is observed indicating a change in the chemical environment via hydride formation [3]. A chemical shift and therefore hydride formation, is observed starting from a thickness of about 25 Å. An identical behaviour is found for Ni(001) (not shown). The change in chemical environment is necessarily due to hydrogen, since the oxygen contamination is negligible for both experiments, with and without hydrogen, (<10% of a monolayer is detected after the experiment) as checked by XPS. A shift of 0.4 eV is comparable to bulk values of YH_2 [3]. The fact that for low coverage we do not find a shift, may be due to the interaction of Y with Ni at this low coverage and, therefore, a much higher hydrogen partial pressure may be needed to induce hydride formation.

In order to study the geometrical arrangement of Y atoms at the surface XPD maps have been recorded. Fig. 2 displays the measurements of various films deposited on Ni(001) and Ni(110). The indicated film thicknesses correspond to the reading on the quartz micro balance. The behaviour on both crystals is similar; relatively thick Y films (Fig. 2(a) and Fig. 2(b)) grown without H_2 do not show any anisotropy. No anisotropy means no ordering, because otherwise some atom–atom directions would be preferentially aligned and therefore we would observe forward-focusing maxima. Also, for thinner films we did not observe ordering. Similarly, relatively thin films (Fig. 2(c) and Fig. 2(d)) deposited under H_2 do not show ordering either. The ring of increased intensity towards the exterior of the map, i.e. for larger polar angles, indicates that Y is sitting at the surface. Such a polar-angle dependence is known to occur for thin overlayers [4]. It can be understood in the following way: as Y atoms sit at the surface, forward-focusing is only possible at grazing emission angles and since there are no atoms above, the measured intensity into the normal direction is weaker. For thicker layers deposited under H_2 (Fig. 2(e) and Fig. 2(f)), however, distinct rings appear going along with the formation of a hydride (Fig. 1). Therefore, we observe H_2 induced ordering. The ordering seems to be slightly better for Ni(110). This might be due to the fact that the film thickness is at the limit of hydride formation as seen from the XPS core-level shift. The rings indicate that there is some preferential orientation with respect to the sample normal. These rings may possibly correspond to randomly oriented fcc(111) domains: the structure of YH_2 is fcc (CaF_2-type) [5] and the angles of nearest-neighbour atoms around the (111) direction correspond to the opening angle of the rings. Note also that for all depositions at room temperature no diffraction spots are detected from LEED which is probing the long-range order.

Ni is an fcc material with a lattice constant of a=3.52 Å and Y is hcp with a=3.65 Å and c=5.74 Å. The difference of the a parameter is not very large but the two materials do have a different structure. The lattice mismatch is even enhanced for fcc YH_2 with a=5.2 Å corresponding to nearest-neighbour distances of 3.67 Å. On the other hand, both lattices are fcc in this case. Probably other aspects, such as heat of formation and surface energies, have to be considered as well for the understanding of this preferential orientation. Note also that for Y deposition at slightly elevated temperatures a quite well-ordered Y–Ni alloy is formed on top of which the hydride is much better ordered. [6]

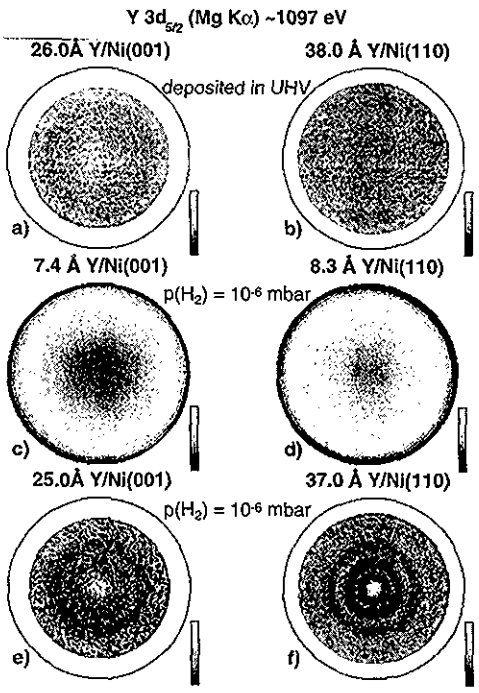

Fig. 2. Y $3d_{5/2}$ X-ray photoelectron-diffraction maps for different Y depositions onto Ni(001) and Ni(110). (a),(b) Thick films deposited without H_2 partial pressure; (c),(d) thin films grown under 10^{-6} mbar H_2 partial pressure; (e),(f) thick films grown under 10^{-6} mbar H_2 partial pressure.

4. Conclusions

From hemispherical X-ray photoelectron diffraction we have found that Y films of different thicknesses deposited at room temperature onto Ni(001) and Ni(110) do not show ordering. Y starts to form a hydride at a thickness of about 25 Å when evaporated under a 10^{-6} mbar hydrogen partial pressure. At the same time such films exhibit a weak ordering in the form of randomly oriented domains preferentially aligned with respect to the surface normal. For thinner films grown under hydrogen partial pressure, not showing hydride formation, no ordering is observed.

Acknowledgments

The authors wish to thank R. Fasel, R. Agostino and T. Pillo, for many stimulating discussions. We also wish to acknowledge the exchange of ideas with Ronald Griessen, Björgvin Hjörvarsson and the other members of the HCM network. Skillful technical assistance was provided by E. Mooser, O. Raetzo, H. Tschopp, Ch. Neururer and F. Bourqui. This project has been supported by the EU-Forschungsprogramm HCM, BBW No. 93.0285, and the Fonds National Suisse pour la Recherche Scientifique.

References

[1] For a review see, e.g., C.S. Fadley, in R.Z. Bachran (ed.), *Synchrotron Radiation Research: Advances in Surface Science*, Plenum, New York, 1989; W.F. Egelhoff Jr., *Crit. Rev. Solid State Mater. Sci., 16* (1990) 213; S.A. Chambers, *Surf. Sci. Rep., 16* (1992) 261; J.

Osterwalder, P. Aebi, R. Fasel, D. Naumović, P. Schwaller, T. Kreutz and L. Schlapbach, *Surf. Sci., 331–333* (1995) 1002.
[2] J. Osterwalder, T. Greber, A. Stuck and L. Schlapbach, *Phys. Rev. B, 44* (1991) 13 764; D. Naumović, A. Stuck, T. Greber, J. Osterwalder and L. Schlapbach, *Phys. Rev. B, 47* (1993) 7462.
[3] A. Fujimori and L. Schlapbach, *J. Phys. C, 17* (1984) 341.
[4] R.G. Agostino, O.M. Küttel, P. Aebi, R. Fasel, J. Osterwalder and L. Schlapbach, *J. Appl. Phys., 80* (1996) 2181.
[5] P. Villars and L.D. Calvert, *Pearson's Handbook of Crystallographic Data for Intermetallic Phases*, Vol. 3, American Society for Metals, Metals Park, Ohio, 1985.
[6] D. Naumović et al., in preparation.